MOEM

Modern Electronic Materials 2023; 9(3): 91–98
DOI 10.3897/j.moem.9.3.111530

Research Article

Charge pumping in solar cell structure

Vitaliy V. Starkov[1], Ekaterina A. Gosteva[2,3]

1 Institute of Microelectronics Technology and High-Purity Materials of the Russian Academy of Sciences, 6 Academician Ossipyan Str., Chernogolovka, Moscow Region 142432, Russian Federation

2 National Research Nuclear University MTPHI, Engineering Physics Institute of Biomedicine, 31 Kashirskoe Highway, Moscow 115409, Russian Federation

3 Peoples' Friendship University of Russia – RUDN University, 6 Miklukho-Maklaya Str., Moscow 117198, Russian Federation

Corresponding author: Ekaterina A. Gosteva (Gos-3@mail.ru)

Received 23 August 2023 ♦ **Accepted** 11 September 2023 ♦ **Published** 30 September 2023

Citation: Starkov VV, Gosteva EA (2023) Charge pumping in solar cell structure. *Modern Electronic Materials* 9(3): 91–98. https://doi.org/10.3897/j.moem.9.3.111530

Abstract

Modern understanding of the material science of semiconductor silicon allowed the authors to propose a new concept of the so-called "charge pumping" in the structures of photovoltaic converters or solar cells. This paper presents theoretical estimates of the rate of separation and collection of light-generated charge carriers in the structures of conventional silicon solar cells and charge-pumped solar cells. Relatively cheaper so-called "solar silicon" of *p*-type conductivity is typically used in the industrial production of solar cells. This type of silicon is particularly prone to the formation of thermodonor centers. Partial or, at higher temperatures (about 400 °C), even complete overcompensation of the hole type of conductivity in the base region may occur as a result of prolonged heating. This paper presents an original model describing the local formation of n^+ regions in the solar cell structure by the so-called "local photon annealing". These regions were named "charge pumps". Experimental data on the formation of n^+ regions as a result of Li diffusion are reported as an experimental confirmation of the theoretical estimations made in this work. Comparative volt-ampere characteristics of experimental charge-pumped photovoltaic converters and conventional solar cells are presented, showing an up to 30% increase in the short-circuit current $J_{s.c}$ for the experimental structures under standard illumination (AM1.5). The proposed technological aspects of charge-pumped photovoltaic converter fabrication deliver a cheap process and can be implemented in the industrial production of solar cells with little effort.

Keywords

energy conversion efficiency, photoelectric converters, photovoltaics, charge pumps, solar cells, local photonic processing, defect-impurity engineering

1. Introduction

The use of solar energy mainly depends on the cost and technology of energy conversion on an industrial scale. The electromagnetic radiation of the Sun that reaches the Earth has components with different wavelengths. About 45% of this radiation is infrared, with wavelengths greater than 0.75 μm, whereas the fraction of ultraviolet radiation (≤ 0.38 μm) constitutes approximately 7%. The maximum intensity of the radiation (~48%) is in the visible, or light, spectrum of the wavelengths (0.38–0.76 μm), which photoelectric converters **(PEC)** use to transform the energy of light into electricity. In the last half-century, several types of solar cells **(SC)** have been developed, among which those based on single-crystal (c-Si) and multicrystalline (mc-Si) silicon have the largest market share due to the relatively high availability of silicon. The relatively low cost of silicon-based SC technologies largely accounts for the increasing production of mc-Si solar cells. The efficiency of SC conversion described by the efficiency factor η reaches 26.7% for conventional ground-based c-Si solar cells. For mc-Si solar cells, η = 26.3% [1] (confirmed single-junction terrestrial cell and submodule efficiencies were measured under the global AM1.5 spectrum (1000 W/m^2) at 25 °C according to IEC 60904-3:2008 or ASTM G-173-03 global standards). For conventional silicon based PECs, the physical limit of efficiency has been practically reached by modern design and technology [2]. At the same time, more and more researchers of new PEC designs report η ≥ 30%. For example, photonic crystal structures of c-Si solar cells [3] have shown an efficiency of 29–30%. These photonic crystals have a thickness of 3–12 μm and consist of inverted-pyramid arrays which, because of their interference properties, significantly concentrate and absorb sunlight and expand the absorbed spectrum. The density $J_{s.c}$ of the short-circuit current produced by solar energy absorption is about 40.49–42.65 mA/cm^2 in the 300–1100 nm wavelength range. If solar energy is concentrated to a level of 20 suns and 150 suns, η can reach 32.5% and 33.5%, respectively.

The PEC design described in [3] has not yet found wide industrial application. Most of the SCs for terrestrial use are made of the cheapest wafers of "solar" silicon and multisilicon which have many structural defects and residual impurities. This leads to spatial inhomogeneity of the recombination-lasing properties in the radiation-absorbing volume of the PEC base. However, solar cells made of "solar" silicon wafers do not show inferior behavior compared to those made of more perfect single-crystal silicon wafers, and in some cases they even exceed the latter ones in the conversion efficiency [4–7].

The large size of SC wafers (~200 cm^2) leads to macroscopic fluctuations of SC parameters in different parts of the front surface thus complicating a conventional assessment of the photoelectric characteristics using the averaged lifetime τ_{ef} and diffusion length L_{ef}. It becomes necessary to clarify the transport mechanisms of light-generated carriers in materials with heterogeneously distributed spatial defects. One possible way to reduce recombination losses in "solar" silicon wafers may be to decrease the separation (collection) time of photogenerated carriers, which can be achieved by reducing the thickness of the SC base region to 3–12 μm [3]. The typical thickness of the surface layer of SC wafers is at least one order of magnitude larger, 100–350 μm, depending on the size of the wafer.

Among the actively developing SC production processes providing for a more efficient use of silicon, the ribbon growth on substrate **(RGS)** technique involves no material losses [4], primarily due to the reduction of silicon waste generated during ingot cutting into wafers, grinding and polishing. However, the RGS-obtained structures have a low lifetime τ_{ef} ~ 0.1 ms because of high concentrations of crystal defects, oxygen, and carbon.

Solar cells fabricated using the RGS method can achieve conversion efficiencies of above 12% and a short-circuit current density $J_{s.c}$ of up to 34 mA/cm^2 under standard illumination, this figure being typical only of good single-crystal silicon SC with much higher minority carrier diffusion lengths. These properties are due to the existence of a three-dimensional network of inversion channels formed by densely packed precipitates around dislocations. Called current collecting channels **(CCC)**, they can collect minority carriers in the main part of a solar cell and direct them to the collector *p–n* junction. Despite the small diffusion length, the volume of collected carriers increases dramatically [4–7]. One or another CCC structure is uncontrollably formed in the RGS process. Various measures are taken to use these structures to increase the SC efficiency.

The collection of charge carriers can be increased by implementing the charge pumping effect in the SC structure [8–11]. The theoretical justification and experimental confirmations of the proposed effect are described below.

2. Theory

The efficiency of photovoltaic converters has a significant impact on the cost of the generated solar electricity. Analysis has shown [12] that an increase in the efficiency of solar cells from 14.4 to 21.5% reduces the cost of electricity generation by 39–41%. In recent years, the efficiency of mass-produced crystalline silicon solar cells has been increasing by about 0.5–0.6% annually.

The main irreversible energy losses in a PEC are as follows:

– reflection of part of the solar radiation from the surface of the converter;

– passage of part of the radiation without absorption (the long wave spectrum region);

– scattering of the excess energy of photons on phonons (the shortwave spectrum region);

– recombination of the generated charge carriers in the volume and on the surface of the PEC;

– internal ohmic resistance of the volume and contacts of the PEC;

– decline of the photo electromotive force (emf) with increasing temperature.

The first three types are optical losses η_{opt}, the remaining three are recombination losses η_{rec}. The total efficiency η can be represented as

$$\eta = \eta_{opt}\eta_{rec}.$$

The efficiency η_{rec} characterizes the fraction of the photocarriers separated (collected) by the *p–n* junction and the created photo emf of the total number of generated electron–hole pairs in the volume of the PEC structure. The maximum value of the optical efficiency is determined by the spectral composition of the solar radiation and the bandgap width of the semiconductor; for single-crystal

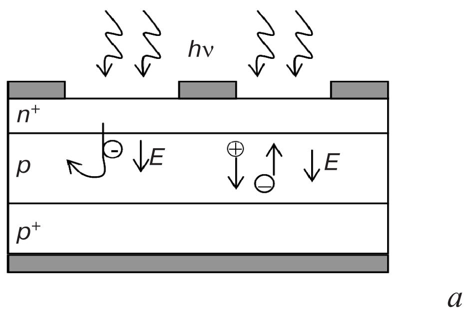

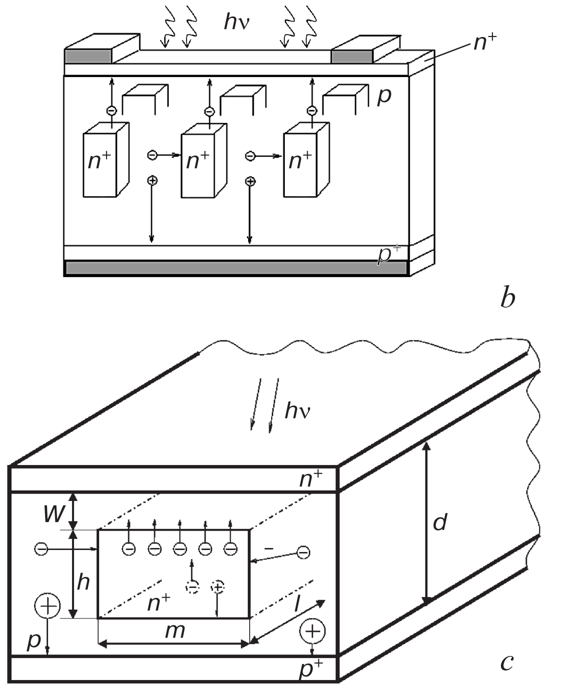

Figure 1. (*a*) Conventional PEC structure, (*b*) "bun with raisins"-type SCCP structure, and (*c*) a fragment of a double-section structure of a strip-type SCCP

silicon η_{max} = 0.29–0.3 in the absence of recombination losses (η_{rec} = 1) [13]. Further increase in the optical efficiency is associated with raising the internal quantum yield of the structure in the blue (shortwave) spectral region and boosting its photoelectric absorption coefficient in the red (long wave) spectral region. Simultaneously, conditions are provided for light trapping due to internal reflections from the front and rear surfaces of the cell. Until recently, the main method of increasing the efficiency of PECs was considered to be decreasing the recombination rate both in the volume (increasing the volume lifetime of nonequilibrium charge carriers τ_{ef}) and on the surface.

The concept of charge pumping, or the controlled formation of so-called "charge pumps" in SC structures [8, 9], is a direction of silicon technology development for industrial production of PECs with an increased efficiency. Schematic structures of conventional solar cells and those based on charge pumping **(SCCP)** are shown in Fig. 1. In comparison with conventional structures, the incorporation of local n^+ regions with a floating potential into the *p*-type base leads to a change in the mechanism of separation and collection of photogenerated nonequilibrium charge carriers. Charge pumps can be metal–semiconductor (Schottky barrier), dielectric–semiconductor, and metal–insulator–semiconductor systems, as well as local heterojunctions, quantum wells, quantum wires, and quantum dots. The main task of charge pumps is to reduce the recombination losses in the volume and on the surfaces of the front and rear electrodes without increasing τ_{ef} (e.g., without perfect silicon crystals obtained using the zone melting method), by reducing the separation time (base flight) in a SC. This allows a more efficient use of cheaper "solar" silicon grown using the Czochralski method or multisilicon with a columnar structure. The electron time of flight in the *p*-type base with charge pumps is determined by the diffusion flight time through the *W* layer for the minority charge carriers (electrons in the case of a *p*-type base) and the drift time of electrons which are the majority carriers in the n^+ region of the thickness *h*. The charge time of the local n^+ region which is determined by the photovoltage generated by the light (Fig. 1 *c*) is $5 \cdot 10^{-11}$ s [10]. Thus, the main inertia is due to the diffusion time through the *W* layer. The thickness of this layer is determined by the location and configuration of the charge pump (n^+ area), which can be tenths or hundredths of the total base thickness *d*. Therefore, in comparison with conventional structures having a similar base size the charge separation time is reduced by one and a half to two orders of magnitude, which significantly reduces the recombination losses. Theoretical estimates [10] show that in a structure in which half of the area (volume) is occupied by charge pumps with $W = 0.1d$ and the other half has the *p*-type base thickness *d*, the efficiency increases from 15% to 21% with the same recombination properties.

An equivalent circuit of a solar cell with n^+ charge pumps (Fig. 2) can be represented as a multi-emitter transistor operating in saturation mode [10]. The current generator J_{L_0} describes the collection of charge carriers in the volume defined by the area S_0 and the thickness *W* of the n^+–*p* junction ("blue" region of light, $\lambda < 0.5$ μm). For a silicon solar cell oriented to fully absorb the "blue" spectrum of solar radiation, $W \gg 3 \cdot 10^{-4}$ cm. Because of simplification of the technology and a smaller influence of the blue spectrum region on the current generators of the charge pumps (J_{L_1}, …, J_{L_i}), we chose an ample value of the thickness, $W = 20 \cdot 10^{-4}$ cm. The function of the recombination current diode (dark current) in the diode equivalent circuit is implemented by the collector

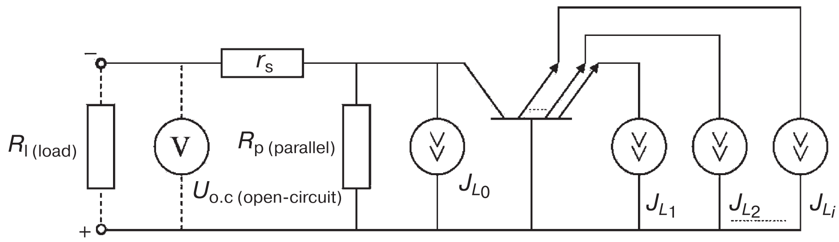

Figure 2. Equivalent substitution circuit of SCCP

junction with a much lower saturation current for the same area, $J_C \sim \tanh(W/L)$. The multi-emitter transistor operates in saturation mode. For a qualitative analysis, all the currents of the generators in the emitter circuit should be summated:

$$J_{L\Sigma} = J_{L_1} + J_{L_2} + \ldots + J_{L_i}.$$

Then the short-circuit current (active mode limit) is

$$J_{s.c} = J_{L0} + \alpha_N J_{L\Sigma},$$

where α_N is the transfer coefficient of the current emitter for normal connection ($\alpha_N > 0.9$).

The open-circuit voltage from the Ebers–Moll model for transistor (double section S_1 and S_2) can be calculated as

$$U_{o.c} = \varphi_T \ln(J_{L0} + \alpha_N J_{L\Sigma})/J_C,$$

where $I_C = S_1 J_C \tanh(d/L_n) + S_2 J_C \tanh(W/L_n)$, $S_1 + S_2 = S_0$ and S_2 is the area of the pumps.

The integral efficiency of a two-section SCCP structure depends on the ratio of the p-type base and charge pump areas in the SC structure. For a standard PEC structure with $d = 180$ µm, area S_0 and $\eta = 15\%$, the efficiency increases to 18.6% after embedding of a charge pump having the area S_2 ($S_2/S_0 = 0.3$) in the base region of the n^+ layer. At $S_2/S_0 = 0.5$, the efficiency increases to 21%, and at $S_2/S_0 = 0.7$, to $\eta = 23.4\%$ [9].

The above estimations indicate that the proposed two-section SCCP structure allows us to improve the efficiency. Similar results were obtained in calculations of an equivalent circuit in which the recombination losses were taken into account via the transfer coefficient:

$$\eta_{rec} = \beta = \mathrm{sch}(W/L).$$

3. Experimental methods

The PEC samples were made of p-type silicon with a resistivity of 7.5 Ωcm, surface orientation (100) and a wafer thickness of 280 µm. The collecting n^+–p junction on the front side and the p^+–p junction on the back side were formed from TEOS-based films using the rapid thermal processing technology **(RTP)** according to a method described earlier [14]. The total area of the experimental PEC structure was 5 × 5 cm^2 (Fig. 3 *a*, *b*). The metallic contacts were formed using standard silk screen printing methods with the same mask for the front and back sides (Fig. 3 *b*, *c*).

The removable photomask for forming strip-type charge pumps in the PEC structure (Fig. 4 *a*) was made from a 3-mm-thick stainless steel plate. The mask

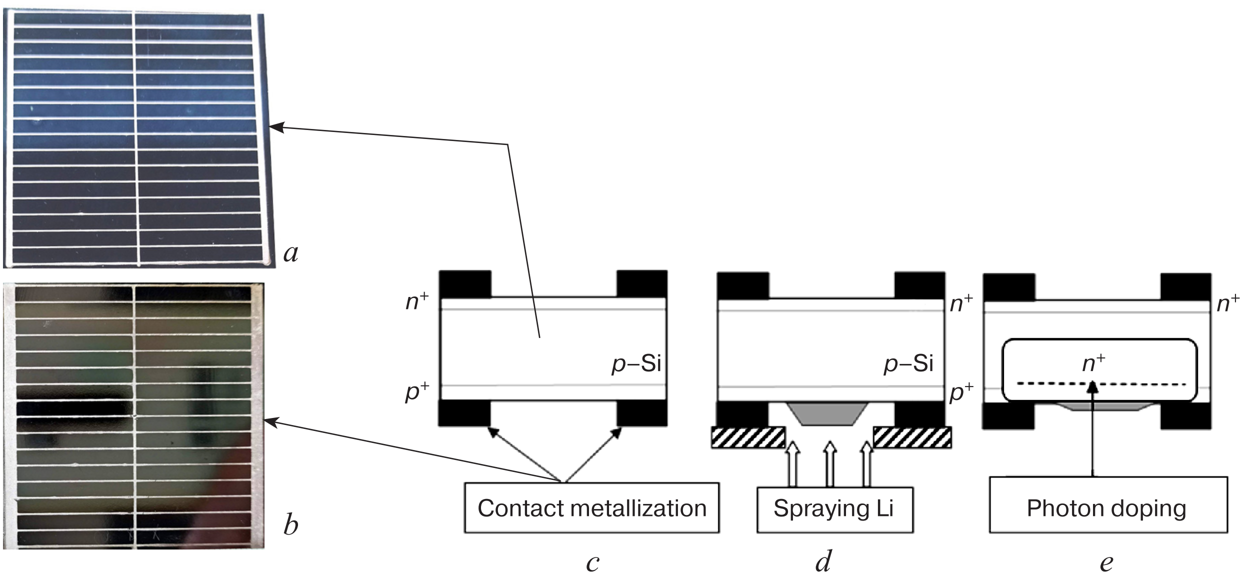

Figure 3. Experimental SC structure: (*a*) front side, (*b*) back side, (*c*–*e*) formation of a charge pump

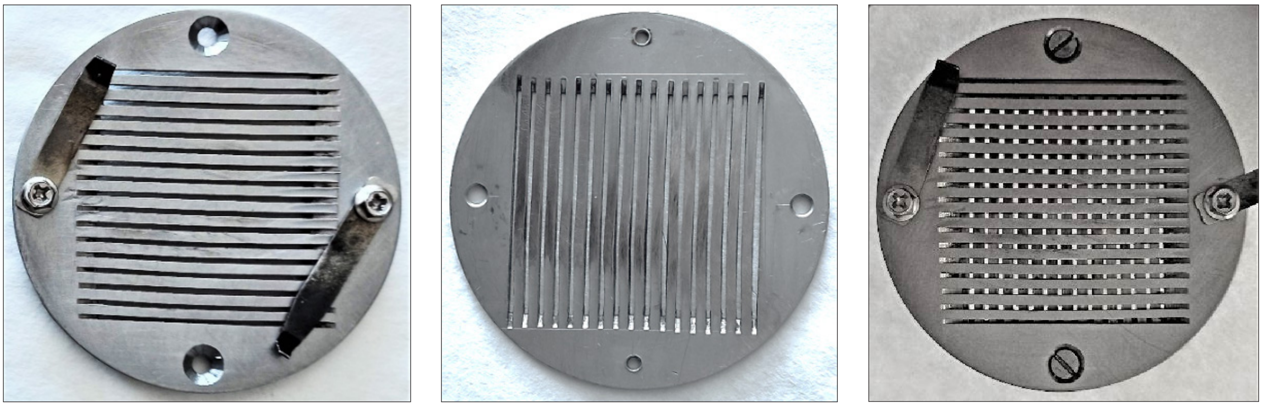

a *b* *c*

Figure 4. Removable overhead photomask: (*a*) front photomask, (*b*) back photomask, (*c*) obtained structure

contained a set of through holes formed by milling, each hole being 1 mm wide and 5 cm long. The distance between adjacent holes was 3 mm which made it possible to place them in the contact metallization gaps of the experimental PECs when they contacted the back side of the PEC structure (Fig. 3 *b*, *c*). This mask design was used for the formation of strip-type charge pumps in the PEC structure (Fig. 3 *c*–*e*).

Two photomasks rotated relative to each other by 90° were assembled together using microscrews (Fig. 4 *c*). The obtained structure with a total thickness of 6 mm had 1 × 1 mm^2 through square holes (Fig. 4 *c*) making it possible to use it for implementing the local photon annealing **(LPA)** mode. The photomask was placed on the SC structure to cover its whole surface and after the end of the light treatment it was removed from the wafer so that the heating temperature of the plate did not exceed 45–55 °C as a result of the treatment. Thus, the photomask also performed the function of a thermal screen that prevented the plate of the solar cell from overheating during the treatment.

The parameters of the finished solar cell wafers were measured using a PASAN900 tester with a pulsed radiation source under standard illumination conditions (AM 1.5 spectrum, illumination intensity 1000 W/m^2, temperature $T = 25$ °C).

The surface temperature of the SC samples was measured using a Term PRO-1200 pyrometer.

4. Results and discussion

The effect of charge pumping on PEC parameters can be demonstrated for the examples of “bun with raisins”-type (Fig. 1 *b*) [10] and strip-type (Fig. 1 *c*) [11] experimental SCs.

4.1. SCCP structures with strip-type charge pumps

Local strip n^+ structures of charge pumps in the *p*-type base of the PEC (Fig. 1 *c*) were formed via photon doping with lithium which was chosen as a donor impurity due to its low injection temperature and recombination of precipitation, leading to suppression of the local recombination rate and hence to an increase in $J_{s.c}$.

The limited diffusion solubility of Li in Si can reach 10^{19} cm^{-3} at about 670 °C [15]. To form n^+ regions, the concentration profile of the *n*-type impurity should be such that not to overcompensate the doping level of the near-contact p^+ layer, and vice versa, it is possible to overcompensate the doping level of the *p*-type base, the doping depth was chosen such that to avoid diffusion overlap of the n^+ areas in the lateral direction and electrical shorting (closure) of the collector and top layers.

Figure 5 shows the experimentally obtained dependences of the depth of *p*–*n* junctions formed by Li diffusion in the experimental PEC structure on the specific power of the halogen lamps and the photon doping time. By setting the specific power of the lamps, we control the process time required to obtain junctions at the desired distance from the charge pump and the collector layer.

The topology of pump arrangement in the *p*-type base should provide for low small series resistance R_s of the rear electrode (Fig. 1 *b*, *c*). To this end, elements having a discrete height (columns) must be located along the perpendiculars to the rear surface, the total thickness of the vertical gaps being (0.1–0.2)d. Current transfer in such a structure is provided by two flows: diffusion of electrons in the volume of the *p*-type base with the thickness *d* and a flow parallel to the electron drift in the n^+ regions of the pump with sequential injection and diffusion through the gap W of the *p*-type base (Fig. 1 *c*).

The strip structures were formed by local deposition of a lithium film on the back side of the plate through a metal mask (Fig. 4 *a*) as shown in Fig. 3 *d*. The mask was in the form of an appropriately sized stainless steel plate with through-slotted strips located between the PEC contact strips on the back side. Lithium was deposited in a vacuum of $1.3 \cdot 10^{-2}$ Pa from a resistive evaporator, the thickness of the metal film being 2 ± 0.5 µm (Fig. 3 *d*). The PEC structure was then removed from the vacuum chamber and loaded in a photon annealing facility [14] for 20 s heating with $P = 37$ W/cm^2 power lamps. As a result, charge pumps were formed in the strip of the

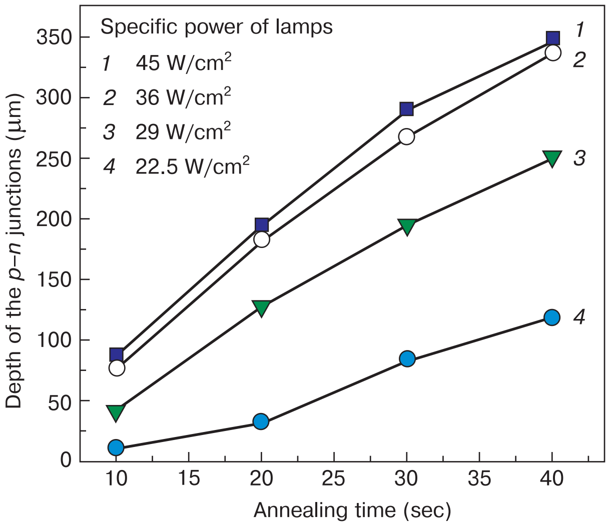

Figure 5. Depth of *p–n* junctions formed by Li diffusion in the experimental PEC structure as a function of specific power of halogen lamps and photon doping (annealing) time. *p*-type Si, surface orientation (100), resistivity $\rho_v = 7.5$ Ωcm

n^+ regions in the base having the *p*-type conductivity. The lithium diffusion depth *h* determined from the depth of the n^+–*p* junction formed in this mode was 158 ± 5 μm (Fig. 3 *c*).

Analysis of the I–V characteristics of the experimental PECs under standard illumination conditions before and after the formation of charge pumps in the SC structure showed an increase in the short-circuit current from $J_{s.c.0} = 274$ mA for the original structure to $J_{s.c} = 354$ mA for the SCCP structure ($\Delta J_{s.c.}/J_{s.c.0} > 0.29$) [10]. The open-circuit voltage U_{oc} of the original structure was 0.565 V, whereas for the SCCPs it was slightly higher, 0.577 V.

Thus, the formation of charge pumps in the strip-shaped n^+ regions of the *p*-type base via Li diffusion leads to an increase in the short-circuit current.

4.2. SCCP with a "raisin bun"-type structure

Rapid thermal annealing **(RTA)** attracts the attention of researchers as a means of solving various defect engineering problems such as annealing of radiation defects, impurity activation after ion implantation into silicon and annealing of thermal donor defects typical of heavily boron-doped Cs–Si wafers [16]. Many studies dealt with the formation of defective oxygen-containing regions in the substrate for subsequent internal gettering processes [17–19]. Using similar processes, researchers [11, 19] have experimentally demonstrated the possibility of creating *n* regions in the wafer volume having *p*-type conductivity.

These conduction regions have been proposed to be used for creation of charge pumps in the *p*-type base region of PECs [8–12].

The process of thermal donor formation is sensitive to the presence of defect clusters, getter layers or inhomogeneities in the silicon structure which generate mechanical stress fields [20, 21].

In this work, charge pumps with a discrete morphology (Fig. 1 *b*) were formed using LPA in a photon annealing unit [14] with a photomask (Fig. 4 *c*) providing spatially discrete light beams. Controlled introduction of charge pumps into local areas of the experimental PEC structure was achieved via local photonic impact with halogen lamps having a specific power of up to 50 W/cm^2.

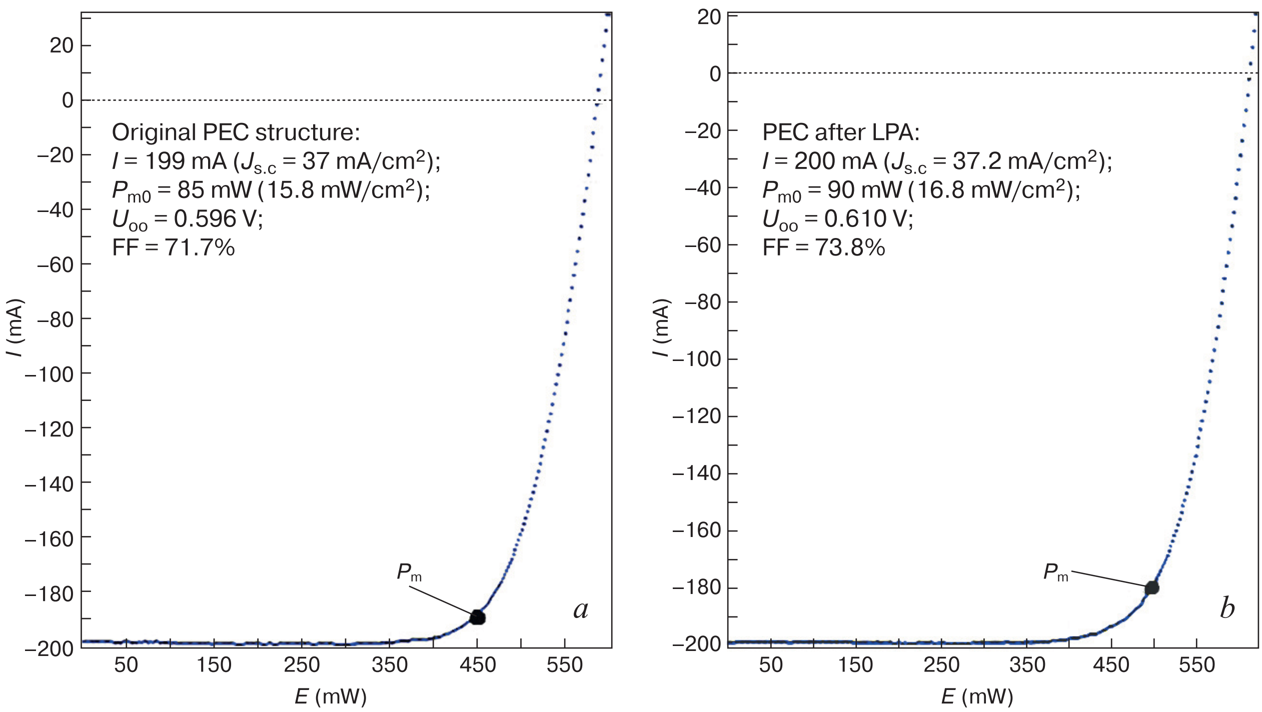

Figure 6. Photonic I–V characteristics of the PEC: (*a*) original structure, (*b*) structure after treatments

Figure 6 shows the photonic I–V characteristics of the PEC having the area S = 5.37 cm^2 and the thickness h = 260 µm. LPA treatment was performed in air at P = 44 W/cm^2 for 9 s. Analysis of the results is shown in the insets of Fig. 6. The dots on the curves mark the maximum power P_m. The power of the PEC samples after the LPA treatment increased, $\Delta P_m/P_{m0}$ = 0.059.

Depending on the photon pulse duration (5–30 s at P = 44 W/cm^2), the change in $\Delta P_m/P_{m0}$ ranged from 3% to 35%, reaching its maximum in the 8–13 s range. At the same time, the maximum increase in the short-circuit current $\Delta J_{s.c.}/J_{s.c.0} \approx 0.37$ was observed for samples with initial efficiencies of lower than 15%. For samples with ≥17% efficiencies and short-circuit current densities $J_{s.c.}$ > 35 mA/cm^2, $\Delta P_m/P_{m0}$ was 7–15%.

The photon pulse duration exceeding 20 s, $J_{s.c}$ and P_m in some samples decreased by more than 50%. Local irradiation forms chains of clusters which turn into conducting n-type channels in the p-type base. Light-generated electrons located at the distance L_{ef} from those channels are driven inside the channels by the electric field and transported by a drift mechanism similar to that for built-in charge pumps formed by doping with n impurities.

5. Conclusions

Modern achievements in the material science of semiconductor silicon provide for further development of theoretical and practical applications of the research results in the production of photoelectric converters. This paper deals with the PEC structure applications of the “charge pumping” concept developed by the Authors.

It is shown that, according to the proposed concept, recombination losses in SC structures can be reduced not only by increasing the volumetric lifetime of nonequilibrium charge carriers τ_{ef}, but also by reducing the separation time of photogenerated carriers via so-called “charge pumps”. This provides for wider application of relatively cheap “solar” silicon wafers in SC production.

A theoretical analysis of the mechanism of photogenerated charge carriers collection in charge-pumped photoelectric converter structures was carried out.

An equivalent substitution circuit of solar cells with n^+ charge pumps was developed which can be represented as a multi-emitter transistor operating in saturation mode.

Experimental studies carried out using the proposed defect-impurity engineering methods confirmed the theoretical conclusions regarding the possibility of increasing the short-circuit current $J_{s.c}$ and the maximum power P_m by forming charge pumps in the structure of the experimental SC.

For the successful implementation of the charge pumping method studied in this paper and hence improving the PEC parameters, it is necessary to take into account the real design and technological features of the manufacture of specific PECs (specific parameters of the silicon wafers used, processes used for their treatment, etc.).

Acknowledgements

The work was supported by the Ministry of Education and Science of the Russian Federation, State task No. 075-01304-23-00.

The study is dedicated to the memory of Professor V.A. Gusev.

References

1. Green M.A., Dunlop E.D., Hohl-Ebinger J., Yoshita M., Kopidakis N., Bothe K., Hinken D., Rauer M., Hao X. Solar cell efficiency tables (version 60). *Progress in Photovoltaics*. 2022; 30(7): 687–701. https://doi.org/10.1002/pip.3595
2. Richter A., Hermle M., Glunz S.W. Reassessment of the limiting efficiency for crystalline silicon solar cells. *IEEE Journal of Photovoltaics*. 2013; 3(4): 1184–1191. https://doi.org/10.1109/JPHOTOV.2013.2270351
3. Bhattacharya S., Baydoun I., Mi Lin, John S. Towards 30% power conversion efficiency in thin-silicon photonic-crystal solar cells. *Physical Review Applied*. 2019; 11(1): 014005. https://doi.org/10.1103/PhysRevApplied.11.014005
4. Lange H., Schwirtlich I.A. Ribbon growth on substrate (RGS) – a new approach to high speed growth of silicon ribbons for photovoltaics. *Journal of Crystal Growth*. 1990; 104.
5. Hahn G., Sontag D., Haessler C. Current collecting channels in RGS silicon solar cells – are they useful? *Solar Energy Materials and Solar Cells*. 2002; 72(1-4): 453–464. https://dx.doi.org/10.1016/S0927-0248(01)00193-3
6. Breitenstein O., Langenkamp M., Rakotoniaina J.P. EBIC investigation of a 3-dimensional network of inversion channels in solar cells on silicon ribbons. *Solid State Phenomena*. 2001; 78–79: 29–38. https://doi.org/10.4028/www.scientific.net/SSP.78-79.29
7. Breitenstein O. Understanding shunting mechanisms in silicon cells: A review. *Proceed. 17th NREL workshop on crystalline silicon solar cells and modules: Materials and processes. Vail, USA;* 2007. P. 61–70.
8. Gusev V.A., Starkov V.V. Solar cells with charge swap. *Proceed. of the 12th Inter. conf. on fundamental and applied studies, development and application of higher technologies in industry. 27–29*

April 2011, St. Petersburg, Russia. St. Petersburg; 2011. Vol. 2. P. 157–158.

9. Gusev V.A. Photoelectric converters based on charge pumps. 2011; (114): 199–203. *Visnik SevNTU. Informatika, elektronika, zv'yazok.* 2011; (114): 199–203. (In Russ.)

10. Gusev V.A., Starkov V.V., Tetersky A.V. Solar cells with the charge pumping: theoretical perspectives and technological aspects of the application. *Izvestiya Vysshikh Uchebnykh Zavedenii. Materialy Elektronnoi Tekhniki = Materials of Electronics Engineering*. 2013; (2): 49–54. (In Russ.). https://doi.org/10.17073/1609-3577-2013-2-49-54

11. Starkov V.V., Gusev V.A., Kulakovskaya N.O., Gosteva E.A., Parkhomenko Yu.N. Formation of charge pumps in the structure of photoelectric converters. *Russian Microelectronics* 2018; 47(8): 608–612. https://doi.org/10.1134/S1063739718080115

12. Woodhouse M., James T., Margolis R., Feldman D., Merkel T., Goodrich A. An economic analysis of photovoltaics versus traditional energy sources: Where are we now and where might we be in the near future? *Proceed. of the 37th IEEE Photovoltaic special. conf. (PVSC). June 19–24, 2011. Seattle, Washington*; 2011. 5 p.

13. Alferov Zh.I., Andreev V.M., Rumyantsev V.D., Solar photovoltaics: trends and prospects, *Semiconductors*. 2004; 38: 899–908. https://doi.org/10.1134/1.1787110

14. Kravchenko V.A., Starkov V.V., Abrosimov N.V., Abrosimova V.N. Diffusion alloying of silicon by boron and phosphorous in conditions of fast thermal annealing. *Elektronnaya tekhnika. Seriya Materialy.* 1989; (4): 20–23. (In Russ.)

15. Reiss H., Fuller C.S., Pietruszkiewicz A.J. Solubility of lithium in doped and undoped silicon, evidence for compound formation. *The Journal of Chemical Physics.* 1956 ;25(4): 650–655. https://doi.org/10.1063/1.1743021

16. Stein H.J., Hahn S.K., Shatas S.C. Rapid thermal annealing and regrowth of thermal donors in silicon. *Journal of Applied Physics.* 1986; 59(10): 3495–3502. https://doi.org/10.1063/1.336820

17. Mezhennyi M.V., Milvidskii M.G., Resnick V.J. Influence of rapid thermal annealing on the specific features of defect generation in silicon wafers during the formation of effective internal getters. *Journal of Surface Investigation. X-ray, Synchrotron and Neutron Techniques*. 2009; 3(4): 612—619. https://doi.org/ 10.1134/S1027451009040223

18. Park J.G., Park H.K., Kwack K.D., Hong J.H. Effect of gas ambient at high temperature rapid thermal annealing on oxygen precipitate formation and crystal originated particle dissolution. *Journal of the Korean Physical Society*. 2001; 39(9(1)): S327–S332. URL: https://www.jkps.or.kr/journal/view.html?uid=4705&vmd=Full

19. Can C., De-Ren Y., Xiang-Yang M., Li-Ming F., Rui-Xin F., Duan-Lin Q. Oxygen precipitation within denuded zone founded by rapid thermal processing in Czochralski silicon wafers. *Chinese Physics Letters*. 2005; 22(9): 2407–2410. https://doi.org/10.1088/0256-307X/22/9/074

20. Emtsev V.V., Andreev B.A., Davydov V.Yu., Poloskin D.S., Oganesyan G.A., Kryzhkov D.I., Shmagin V.B., Emtsev V.V., Misiuk A., Londos C.A. Stress-induced changes of thermal donor formation in heat-treated Czochralski-grown silicon. *Physica B: Condensed Matter*. 2003; 340–342: 769–772. https://doi.org/10.1016/j.physb.2003.09.118

21. Starkov V.V., Gosteva E.A., Irzhak D.V., Roshchupkin D.V. Study of the effect of local photon annealing on stress in silicon wafers. *Modern Electronic Materials*. 2019; 5(3): 141–144. https://doi.org/10.3897/j.moem.5.52500